

# **EXPERIMENTAL AND NUMERICAL STUDIES OF GAS INJECTION IN FRACTURED CARBONATES: PRESSURE AND COMPOSITIONAL EFFECTS**

Jon K Ringen<sup>(1)</sup>, Vidar Haugse<sup>(1)</sup>, Lars Høier<sup>(1)</sup>, Lars Inge Berge<sup>(1)</sup> and Jules Reed<sup>(2)</sup>  
<sup>(1)</sup>Statoil-Norway, <sup>(2)</sup>Reslab-Norway

*This paper was prepared for presentation at the International Symposium of the Society of Core Analysts held in Toronto, Canada, 21-25 August 2005*

## **ABSTRACT**

The purpose of the three experiments described in this paper was to investigate gas injection in fractured carbonate reservoirs, focusing on the effect of capillary continuity, re-pressurization by equilibrium gas, and injection of non-equilibrium gases. A composite core made from carbonate core material from a Middle East reservoir was placed vertically in a core holder with free space in the annulus between core and cell body. The core was saturated with oil phase and surrounded by gas. Synthetic fluid systems consisting of C1, C3, and nC10 were used. Pressure and temperature were selected to give proper IFT vs. capillary pressure and block height.

Series of gas injections were performed on the composite core as a single block, with all plugs in capillary contact, and with two types of barriers in the middle of the composite core, establishing two blocks. Experimental data from the study include oil and gas production data, and gamma attenuation in-situ saturation profiles. Capillary pressure and relative permeabilities were measured on plugs similar to those used in the composite core.

The experiments showed a significant effect of increasing the pressure from 200 to 240 bars, especially for the two block configuration. The oil recoveries from equilibrium gas injection with a barrier in the core were significantly lower than in the experiment with all plugs in contact. An experiment with a thin, perforated barrier gave similar poor oil recovery as with a thick barrier, indicating poor capillary contact in both cases. Injection of a rich non-equilibrium gas recovered almost 100 % of the oil, whilst injection of lean non-equilibrium gas also improved the oil recovery.

A compositional reservoir simulation model was set up to simulate the experiments. The simulation model gave a good match of the experimental results after history matching.

## **INTRODUCTION**

Several large fractured carbonate reservoirs have been produced by depletion, resulting in moderate oil recovery factors. Large amounts of oil may be trapped in the matrix blocks by capillary forces due to expansion of an initial or secondary gas cap. An efficient IOR method for such reservoirs could be to increase the reservoir pressure by gas injection. The reduced interfacial tension would improve the oil recovery factor with increasing

pressure. Further improvements may be obtained by compositional effects if a non-equilibrium gas is injected. In the following, some papers relevant for the main topics of this paper are reviewed.

### **Capillary Continuity/Fracture Capillary Pressure**

The petroleum literature contains numerous papers related to capillary continuity/fracture capillary pressure, as this may have a major influence on oil recovery in fractured reservoirs<sup>1</sup>. The maximum fracture capillary pressure must be as high as the matrix capillary pressure to obtain gravity/capillary equilibrium (Gilman and Kazemi<sup>2</sup>).

Saidi<sup>1</sup> argued that capillary continuity could not be realized if the fracture aperture was above 0.05 mm. The experiments of Horie et al.<sup>3</sup> showed that the liquid recovery for matrix blocks separated by 0.3 mm thick aluminium shims were much lower than when the matrix blocks were in direct contact or separated by coarse or fine sand (but a vertical stress had to be applied to obtain high recovery in the case with coarse sand separating the blocks). Based on gravity drainage experiments, Firoozabadi and Markeset<sup>4</sup> concluded that the fracture liquid flow is mainly film flow for gas-oil gravity drainage and that the rate of drainage across a stack of matrix blocks is very sensitive to the fracture aperture. More recent experiments by Sajadian et al.<sup>5</sup> showed that increasing the space between matrix blocks from 0.5 mm to 2.6 mm had a significant negative impact on the recoveries. A formula for critical aperture size was suggested (i.e. effective capillary continuity through liquid bridges if the fracture aperture is less than the critical value), but it is not clear if this formula is consistent with experimental results.

### **Re-pressurization**

Saidi<sup>6</sup> presented the performance from re-pressurization of the Haft Kel field, including the background for this gas injection project and modelling issues. According to this analysis, the combination of no capillary continuity and reduced interfacial tension at higher pressure are main factors for the successful gas injection project in this field. Re-pressurization is currently used on several other fields, while little experimental work has been presented in the literature.

### **Non-Equilibrium Gas Injection**

Several experimental studies on non-equilibrium gas injection in fractured reservoirs are reported in the literature, e.g. miscible displacement studies by Firoozabadi and Markeset<sup>7</sup>, diffusion dominated experiments by Morel et al.<sup>8</sup>, dry gas injection in fractured chalk by Øyno et al.<sup>9</sup>, and CO<sub>2</sub> gravity drainage experiments by Li et al.<sup>10</sup>. Separate numerical studies on some of the experiments were also presented, e.g. Firoozabadi and Tan<sup>11</sup> and Hu et al.<sup>12</sup>. The IOR potential by non-equilibrium gas injection was further investigated in a simulation study by Uleberg and Høier<sup>13</sup>, showing very high recovery factors even when miscibility was not achieved.

Field cases with non-equilibrium gas injection in fractured reservoirs are also reported, e.g. the Nitrogen injection project in the Cantarel complex<sup>14</sup> and tertiary CO<sub>2</sub> injection in the Midale field<sup>15</sup>.

## **EXPERIMENTS**

### **Cores and Equipment**

Dolomitic carbonate cores from a Middle East reservoir were used in the experiments. The objective was to build a long composite core which could be divided into two distinct block systems (high and low permeability) with sufficient height to allow gravity drainage in both. The selection was based on a combination of CT images, porosity, and permeability properties.

Table 1 provides an overview of core sample properties; displaying individual, block and composite properties. The samples were ordered by decreasing permeability from top to bottom.

The experiments were performed in a modified reservoir conditions core holder which allows the passage of gamma radiation for measurement of in situ saturation monitoring (ISSM), at conditions up to 700 bar and 150°C. Modifications were made to allow a composite core to be loaded without the confines of a rubber sleeve. Metal rods were manufactured with adjustable peak nubs to aid core support and also direct any produced oil back towards the core, thus preventing a wick-like flow down the supporting rods. The annular space surrounding the composite core thus acts as the fracture system. The dimensions of the core holder were; internal diameter: 49 mm, internal length: 640 mm. The pore volume of the empty core holder, measured by helium injection, was 1158 cm<sup>3</sup>, providing an annular space of approximately 590 cm<sup>3</sup>, once core and supporting apparatus were loaded.

Figure 1 displays the composite core loaded into the supporting rods, including a schematic of the system. A peak cap allowed for centring of the core and also contained a spring loading system to provide a small pressure to assist capillary contact.

In addition to the long core, twin samples were measured with respect to capillary pressure (Hg-injection and g/w centrifuge drainage) and relative permeability (gas/water centrifuge drainage). These results were used both in simulations during the planning phase of the long core experiments and in the history matching of the experiments.

### **Fluids**

The long core experiments were performed without an irreducible water phase present (Swi). This was decided to be able to efficiently re-establish the initial conditions (So=1) for new experiments. Also the gamma in-situ saturation determination system would be very sensitive to any change in water saturation (movement or drying out). The lack of a

low stationary water phase is not believed to alter the main processes in this study, but could have an impact on the results.

It was decided to use a three-component fluid system in the experiments; methane (C1), propane (C3) and normal-decane (nC10). Such fluid systems are easy to prepare, and the selection of appropriate fluids/pressure/temperatures for a particular experiment may be supported by Equation-of-State (EOS) calculations. For our experiments it was important to select fluids with reasonable IFTs, i.e. a moderate oil recovery at the lowest pressure and potential for improved recovery at the highest pressure.

Fluid properties were estimated from a three-component SRK EOS. The volume shifts and parachors of the final EOS were tuned to measured oil and gas densities and IFTs (see Table 2), while the assumed fluid compositions were based on EOS calculations. Fluid compositions and EOS parameters used in the compositional reservoir simulation model are shown in Table 3 and Table 4. The minimum miscibility pressure with rich gas was estimated to be about 285 bar by slimtube simulations with proper elimination of numerical dispersion, i.e. all experiments are performed at immiscible conditions.

### **Experimental Methods**

The selected individual core samples were loaded into the rod support system, in the ordering sequence provided in Table 1. Capillary contact was aided by using a sandwich of tissue paper and decane infused kaolinite paste. A spring loaded, peak cap was placed at the top of the core and fixed in place. The position of the individual plugs was recorded to ensure consistency through all experiments.

Three gas injection series were performed on the following core arrangements:

1. All plugs in capillary contact - making them a single block.
2. With a 8 mm thick Teflon barrier inserted between the plugs in the middle of the composite core, creating two blocks - presumably not in capillary contact.
3. With a thin, 0.125 mm, perforated disk made of tin replacing the Teflon barrier - to create possible capillary contact between the two blocks.

The assembly was loaded into the modified core holder and the pore volume was measured by helium injection. The system was heated to 40°C and a small vacuum was drawn. Methane was drawn in under vacuum before the system was charged with the 200 bar equilibrium oil and brought to a pressure of 340 bar (above expected saturation pressure). To ensure that the core holder was fully charged, equilibrium oil was flooded at a low rate from bottom to top. The gas injection into the top was started when the gamma counts were stable.

Experiment 1 (one long core - single block) and Experiment 2 (two blocks w/Teflon barrier) consisted of three stages:

- A. Injection of equilibrium gas at 200 bar and medium IFT.
- B. Followed by equilibrium gas at 240 bar and low IFT.

C. Followed by a rich non-equilibrium gas (90 mol-% C1, 10 mol-% C3).

For Experiment 3, the first stage was followed by injection of 100 % C1 at 200 bars.

Each stage began by a rapid injection ( $15\text{cm}^3/\text{min}$ ) to displace the contents of the annular space, followed by a slower rate injection over several days.

Experiment 1 – stage A was performed at a rate of  $0.025\text{cm}^3/\text{min}$  and ran for 7 days. Pressure was then increased by shutting in the system and continuing to inject 200 bar equilibrium gas until 240 bar was achieved. 240 bar equilibrium gas was then injected at a high rate to displace the annular space. Injection rate was reduced to  $0.025\text{cm}^3/\text{min}$  for approximately 7 days. The non-equilibrium gas was then injected by the same procedure; 1460 ml injected. Experiment 2 was performed in the same manner for stages A and B. However, the non-equilibrium gas was injected at a higher rate to observe if this would affect production rate; 3854 ml injected. In Experiment 3, the 200 bar equilibrium gas injection was followed by injection of 1810 ml of methane at 200 bar.

Measurement of production was performed by flashing the effluent to ambient conditions and recording the volume of oil recovered in a graduated separator. Production volumes at the experimental conditions were calculated, accounting for volume expansion factor for each system and deducting the volume of injected nC10, the assumption being that the collected oil contained nC10 only.

### **Experimental Results and Discussion**

A summary of results can be found in Table 5. The increase in pressure (200 to 240 bar) and subsequent decrease in IFT provided additional production in both experiments. The experiments also show a significantly reduced oil recovery due to the capillary break/barrier in experiments 2 and 3.

Figures 2-4 provide saturation profiles gained from gamma in situ saturation monitoring (ISSM) for all experiments. The single block experiment (Figure 2) can be seen to drain the core at 200 bar from top until the capillary threshold is reached. The observed  $S_o=1$  in bottom of plug 4 is not easy to explain. After increase of pressure to 240 bar and lower IFT a more efficient drainage and lower threshold was achieved. The apparently increase in  $S_o$  at the top of the core is probably due to the technical problems with the ISSM in that experiment. The effect of the barrier in the middle of the long core are clearly visible in Figures 3 and 4; only the top of each block is drained and more efficient in the top block due to higher permeability and porosity.

The profiles agree well (in trend) with the modelled data and clearly show the effect of capillary continuity and discontinuity. The saturation profiles display similar trends to the mass balance and modelled data. However, certain stages exhibited distinct differences, making the ISSM data possibly more qualitative than quantitative. The major differences were observed in Experiment 1 and the methane injection of Experiment 3.

Temperature control difficulties observed during Experiment 1 may have affected the gamma attenuation by 5-10 saturation percent. The non-equilibrium gas injection altered the oil composition and hence oil attenuation. But saturation calculation was based upon a calibration scan of the 2 fluid phases assuming constant attenuation. Therefore, the changing attenuation will produce an error in the calculated saturation.

Experiment 3 was performed with a thinner capillary break to attempt to investigate if contact could be made between blocks by film flow. It was considered that 0.125 mm may allow film flow in the system. However, although the tin disc was 0.125 mm the actual break was probably somewhat larger due the uneven surface of the core face.

The production of oil and change in recovery (1-So) are plotted in Figures 5-7. The different stages in the experiments are indicated by vertical lines. In general there is a good match between the gamma ISSM data and the mass balance (produced liquid). The increased injection rate of the non-equilibrium gas during Experiment 2 was seen to have a significant effect on the production rate, with Experiment 1 taking 15-16 days to stabilise and Experiment 2 stable after only 2 days. The low residual saturations were confirmed by extraction of the plugs after each experiment.

## **NUMERICAL SIMULATION OF THE EXPERIMENTS**

A compositional reservoir simulation study was performed to investigate if the main characteristics of the measurements could be reproduced by a simulation model. Also, a successfully history matched simulation model can be used to scale the laboratory results to scenarios that are closer to real situations, e.g. changing geometry, fluids, and injection volumes. In the following, the construction of the simulation model and the history matching of the results are discussed.

### **Construction of Compositional Reservoir Simulation Model**

A black oil model could have been used to simulate the first part of the experiments, but a compositional model is required for the last part. A commercial compositional reservoir simulator<sup>16</sup> was used in this study.

A radial grid was used, where each plug was assumed to be homogeneous and consisted of 10x1x10 grid blocks. The fracture surrounding the plugs was represented with the same vertical resolution as the plugs, but with a single set of grid blocks in the radial direction. The fractures above/below the plugs were represented by two numerical layers. Linear relative permeabilities, no capillary pressure, unity porosity, and permeability of 100 D were used for the fractures. The fracture created by the tin plate in the last experiment was also represented by a single numerical fracture layer in the simulation model. Gas was injected in the fracture above the plugs and oil and gas was produced from the fracture at the bottom. The injector and producer were controlled by pressure and reservoir volume rate, respectively.

Diffusion coefficients were estimated from the extended Sigmund correlation<sup>17</sup>. Simulations of the experiments with rich gas used diffusion coefficients based on the oil/rich gas compositions at 240 bar, while oil/dry gas compositions at 200 bar were used for the last experiment. Table 6 summarizes the diffusion coefficients used in simulations.

The relative permeability and capillary pressure curves were based on plugs similar to those used in the gas injection experiments. Corey exponents for oil and gas relative permeabilities were set to 3 and 2, respectively. A common J-function was initially used for all plugs, but with individual residual oil saturation for each plug. The residual oil saturation varied from 11.4 % for the top plug to 22.7 % for the bottom plug as linear function of permeability. Relative permeabilities and J-function are illustrated in Figure 8. IFT was also used to scale the capillary pressure. A potential problem with simulation of gas injection in fractured reservoirs is that the capillary entry pressure depends on pressure and gas and oil compositions. Reservoir simulators typically assumes a fixed or pressure-dependent reference pressure IFT for single-phase matrix blocks, i.e. there may be a discontinuity in capillary entry pressure as the first gas invades a matrix block. To avoid these problems in the current study, the J-function was set to zero at no gas saturation, followed by a rapid increase in the J-function for gas saturations less than 1 %.

### **History matching**

Some modifications of input parameters to the simulation model were required to achieve a match to the measured data. For this model, multipliers on the capillary pressure curves for each plug were used as history matching parameters. The estimated oil saturations from gamma measurements were used in a qualitative way in the tuning of the simulation model. A good match to the experiments was achieved by using the following multipliers on the capillary pressure curves for the upper five plugs: 0.5, 0.7, 0.65, 0.4, and 0.55. No modifications were made for the three bottom plugs. Corey exponents were unchanged.

The simulation results for Experiment 1 are shown in Figure 9, illustrating that the match to the average oil saturation at the end of each experimental phase is good. The details of each phase are not reproduced by the simulator, but the simulation model captures the main characteristics of the experiment. Note from the plots of oil saturation vs. depth that capillary-gravity equilibrium is not reached for the gas injection at 240 bar, e.g. the oil saturation in plug 4 is decreasing with depth. Only minor amounts of oil are left in the bottom plug at the end of the rich gas injection when diffusion is included in the simulations, while the simulation without diffusion produces too little oil during the rich gas injection period. The rich gas enters the matrix also in simulations without diffusion because of the gravity potential created by the density difference between the rich gas and equilibrium gas.

Simulations of the second and third experiment are shown in Figure 10 and Figure 11. Again, the simulation models give an acceptable match of the experiments. Note that for the lean gas injection, Figure 11 indicates that the simulation case without diffusion

seems to give the best match to the experimental data. However, the experimental data in this figure is based on measured oil production at standard conditions (i.e. mainly nC10), while a significant recovery mechanism in the simulation model is vaporization of C3 (in fact, the oil in the top of the core at the end of the experiment consists only of C1 and nC10). It is therefore believed that the simulation with diffusion is closer to the laboratory results also for experiment 3.

## CONCLUSIONS

The conclusions from our experimental and numerical studies are:

1. Oil recovery by gas injection was significantly lower when flow obstructions were placed between the plugs than in the experiment with stacked plugs. Even a 0.125 mm perforated tin plate gave a discontinuity in the capillary pressure.
2. Re-pressurization by gas injection resulted in significant oil production in all cases. The increase in oil recovery factor was highest in the case with barrier between two plugs.
3. Practically all oil could be recovered by injection of rich non-equilibrium gas, where vaporization and reduced IFT are key factors for increased and accelerated recovery from rich gas injection compared with equilibrium gas injection. Injection of lean gas also improved the oil recovery significantly.
4. History matching the compositional reservoir simulation provided a good match of all experiments. The numerical simulations of the experiments indicate that diffusion improves the oil recovery by non-equilibrium gas at this scale.

## REFERENCES

1. Saidi, A.M.: Reservoir Engineering of Fractured Reservoirs, TOTAL Edition Press, (1987).
2. Gilman J.R and Kazemi, H "Improvements in Simulation of Naturally Fractured Reservoirs", SPE Journal, (Aug. 1983), p. 695-707, SPE 10511.
3. Horie, T., Firoozabadi, A., and Ishimoto, K. "Laboratory Studies of Capillary Interaction in Fracture/Matrix Systems", (1990), SPE 18282.
4. Firoozabadi, A. and Markeset, T. "Fracture-Liquid Transmissibility in Fractured Porous Media", (1993), SPE 24919.
5. Sajadian, V. A., Danesh, A., and Tehrani, D.H. "Laboratory Studies of Gravity Drainage Mechanism in Fractured Carbonate Reservoir - Capillary Continuity", (1998) SPE 49497.
6. Saidi, A.M. "Twenty Years of Gas Injection History into Well-Fractured Haft Kel Field (Iran), presented at the International Petroleum Conference & Exhibition of Mexico held in Villhemos (1996), SPE 35309.
7. Firoozabadi, A. and Markeset, T.I. "Miscible Displacement in Fractured Porous Media: Part I-Experiments", presented at the SPE/DOE Ninth Symposium on Improved Oil Recovery held in Tulsa, Oklahoma, USA (1994), SPE 27743.

8. Morel, D., Bourbiaux, B., Latil, M., Thiebot, B. "Diffusion Effects in Gasflooded Light-Oil Fractured Reservoirs", *SPE Advanced Technology Series*, (June 1993), p. 100-109, SPE 20516.
9. Øyno, L, Uleberg K., Whitson C.H. "Dry Gas Injection in Fractured Chalk Reservoirs - An Experimental Approach", presented at the International Symposium of the Society of Core Analysts held in San Francisco, California (1995), SCA1995-27.
10. Li, H., Putra, E., Schechter, D. S., and Grigg, R. B. "Experimental Investigation of CO<sub>2</sub> Gravity Drainage in a Fractured System", presented at the SPE Asia Pacific Oil and Gas Conference and Exhibition in Brisbane, Australia (2000), SPE 64510.
11. Firoozabadi, A. and Tan, J.C.T. "Miscible Displacement in Fractured Porous Media: Part II-Analysis", presented at the SPE/DOE Ninth Symposium on Improved Oil Recovery held in Tulsa, Oklahoma, USA (1994), SPE 27837.
12. Hu., H, Whitson C.H., and Qi, Y. "A Study of Recovery Mechanisms in a Nitrogen Diffusion Experiment", presented at the 6<sup>th</sup> European Symposium on Improved Oil Recovery in Stavanger, Norway (1991).
13. Uleberg, K, and Høier, L. "Miscible Gas Injection in Fractured Reservoirs", presented at the SPE/DOE Thirteenth Symposium on Improved Oil Recovery held in Tulsa, Oklahoma, USA (2002), SPE 75136.
14. Rodriguez, F., Sanchez, J.L., and Galindo-Nava A. "Mechanisms and Main Parameters Affecting Nitrogen Distribution in the Gas Cap of the Supergiant Akal Reservoir in the Cantarell Complex", presented at the SPE Annual Technical Conference and Exhibition, Houston, Texas (2004), SPE 90288.
15. Beliveau, D., Payne, D. A., and Mundry, M." Waterflood and CO<sub>2</sub> Flood of the Fractured Midale Field", *SPE Journal of Petroleum Techn.* (Sept. 1993), p. 881-817.
16. ECLIPSE Reference Manual 2004A, Schlumberger Information Systems.
17. da Silva, F.V. and Belery, P. "Molecular Diffusion in Naturally Fractured Reservoirs: A Decisive Recovery Mechanism", presented at the SPE Annual Technical Conference and Exhibition, San Antonio, TX, USA (1989), SPE 19672.

## **ACKNOWLEDGEMENT**

We would like to thank Rolf S Johansen for conducting most of the experimental work and Marcel Lanchmans and Matts Devik for the equipment design, all Reslab employees. We also thank Statoil for financing this study and allowing the results to be published.

**Table 1: Basic core properties – individual and composite core.**

TOP → BOTTOM

Block Number	Block 1				Block 2				
Sample ID	1	2	3	4	5	6	7	8	
Length (cm)	7.08	6.23	7.85	5.02	7.81	8.18	4.94	4.85	
Pore Volume (cm <sup>3</sup> )	23.4	20.6	27.4	17.8	20.5	19.3	14.8	12.4	
Porosity (frac)	0.303	0.309	0.320	0.321	0.240	0.218	0.268	0.231	
Grain Density (g/cc)	2.74	2.83	2.84	2.84	2.84	2.85	2.84	2.83	
K <sub>L</sub> (mD)	223	191	182	116	62.6	46.1	43.5	41.8	
<b>Composite Core Data</b>									
	Block 1				Block 2				Total
Length (cm)	26.18				25.78				51.96
Pore Volume (cm <sup>3</sup> )	89.1				67.0				156.2
Porosity (frac)	0.313				0.237				0.275
Average K <sub>L</sub> (mD)	178				48.5				113

**Table 2: Measured interfacial tensions and densities at 40°C.**

Pressure (bar)	IFT (mN/m)	Oil density (g/cc)	Gas density (g/cc)
200	2.35	0.560	0.184
240	1.20	0.534	0.214

**Table 3: Molar fluid compositions for the three-component EOS.**

Component	Oil 200 bar	Eq. gas 200 bar	Eq. gas 240 bar	Rich gas	Lean gas
C1	0.57820	0.94097	0.93311	0.90	1.0
C3	0.11182	0.05209	0.05402	0.10	0.0
nC10	0.30998	0.00694	0.01287	0.00	0.0

**Table 4: Parameters for the three-component SRK EOS.**

Component	Mw	Tcrit K	Pcrit bara	Zcrit	AF	Vshift	Parachor	BIP C1
C1	16.0429	190.60	46.0015	0.28737	0.008	0.201918	16.870	-
C3	44.0968	369.80	42.4552	0.28029	0.152	0.204458	151.900	0.0000
nC10	142.2853	617.60	21.0756	0.24748	0.490	0.146283	417.100	0.0411

**Table 5: Summary of the results from the three gas injection programmes.**

		Experiment 1 Single Core	Experiment 2 8 mm Break	Experiment 3 0.125 mm Break
<b>200 bar Equilibrium Injection</b>				
Oil Production	(cm <sup>3</sup> )	75.9	29.1	28.9
Oil Saturation – Mass Balance	(frac)	0.514	0.814	0.815
Oil saturation - Gamma	(frac)	0.679	0.854	0.829
<b>240 bar Equilibrium Injection</b>				
Oil Production	(cm <sup>3</sup> )	86.0	59.5	
Oil Saturation – Mass Balance	(frac)	0.449	0.682	
Oil saturation - Gamma	(frac)	0.562	0.712	
<b>240 bar Non-Equilibrium Injection</b>				
Oil Production	(cm <sup>3</sup> )	154.3	160.5	
Oil Saturation – Mass Balance	(frac)	0.012	0.035	
Oil saturation - Gamma	(frac)	0.038	0.021	
<b>200 bar Methane Injection</b>				
Oil Production	(cm <sup>3</sup> )			47.7
Oil Saturation – Mass Balance	(frac)			0.695
Oil saturation - Gamma	(frac)			0.458

**Table 6: Diffusion coefficients for oil and gas used in compositional reservoir simulation models.**

Component	Experiment 1 and 2		Experiment 3	
	Do cm <sup>2</sup> /s	Dg cm <sup>2</sup> /s	Do cm <sup>2</sup> /s	Dg cm <sup>2</sup> /s
C1	2.15E-05	3.61E-04	2.38E-05	3.35E-04
C3	1.99E-05	3.61E-04	1.98E-05	5.25E-04
nC10	1.60E-05	1.53E-04	1.74E-05	2.46E-04

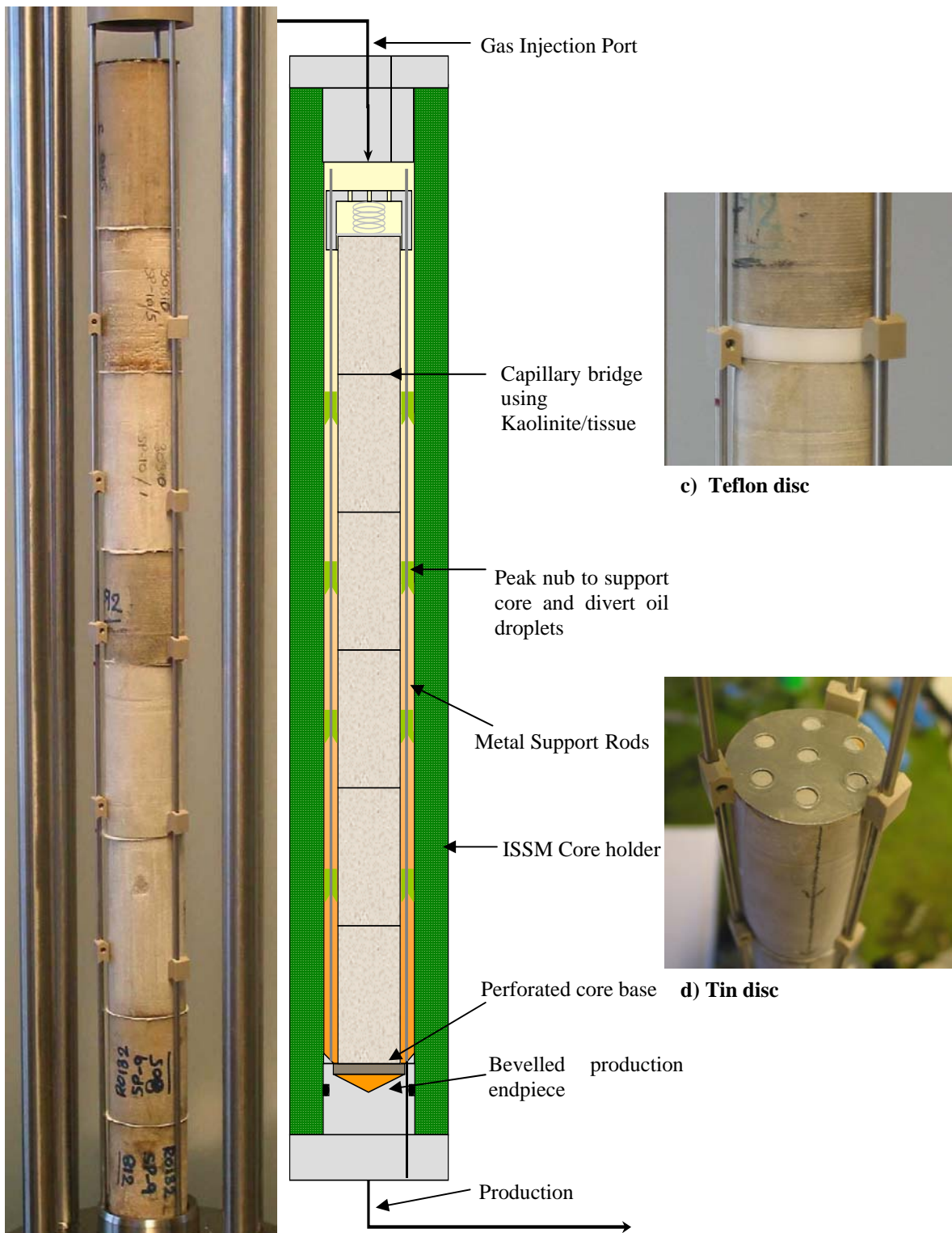


Figure 1a) . Composite Core Sample. b) Schematic Diagram.

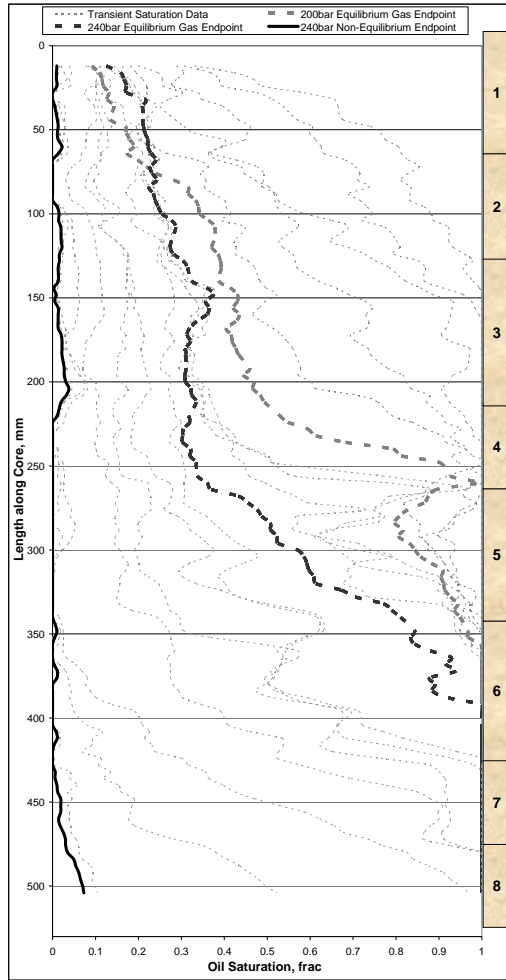


Figure 2: Gamma saturation plot of gas injection into the single long core experiment.

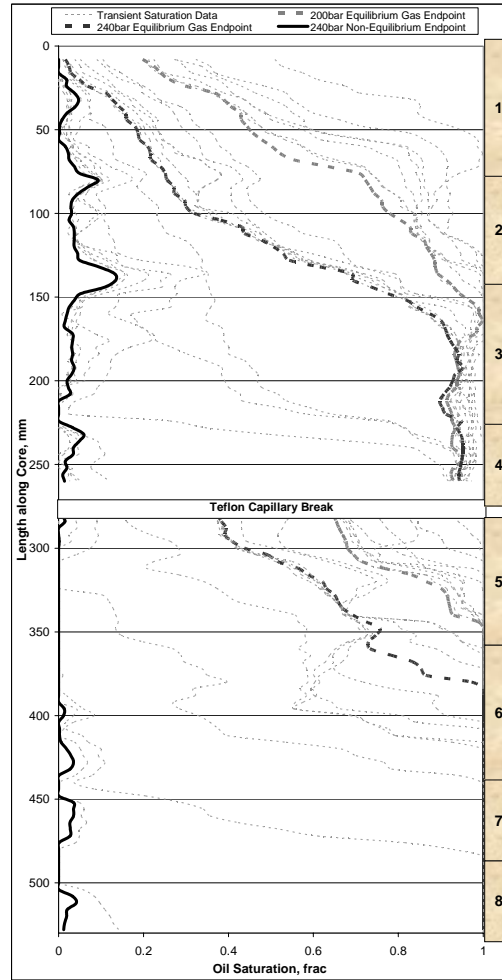


Figure 3: Gamma saturation plot of gas injection. 2 block system w/ 8 mm Teflon disc.

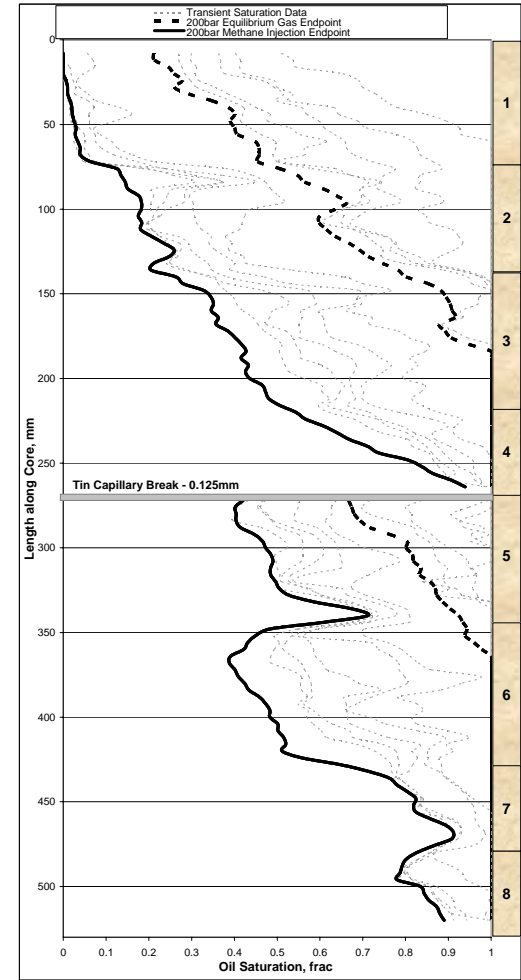


Figure 4: Gamma saturation plot of gas injection. 2 block system with a 0.125 mm punctured tin disc.

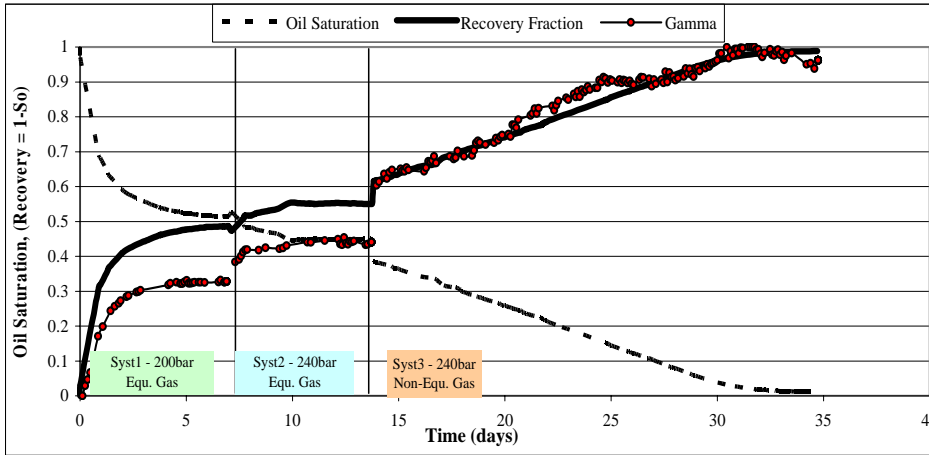


Figure 5: Experiment 1. Production as a function of time – gas injection into a single core system.

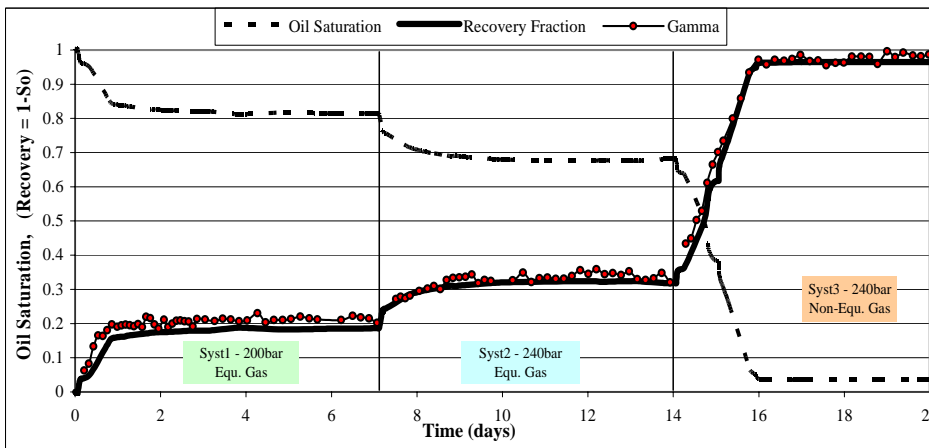


Figure 6: Experiment 2. Production as a function of time – gas injection into a 2 block system; 8 mm Teflon disc as the capillary break.

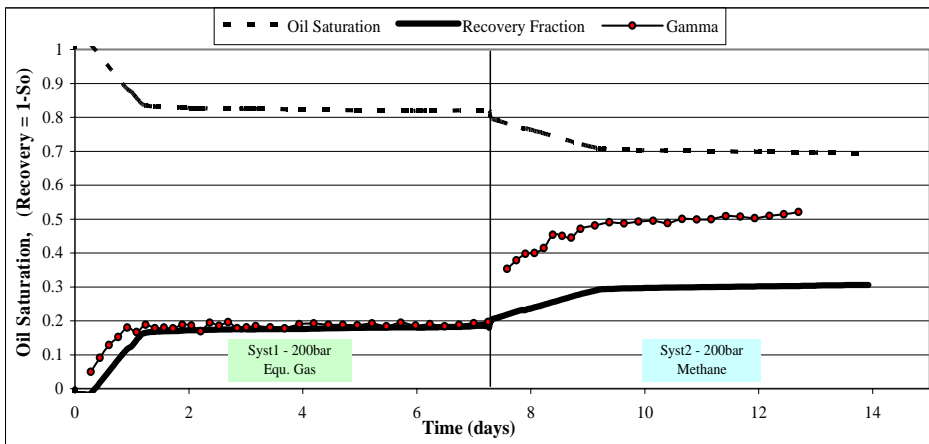


Figure 7: Experiment 3. Production as a function of time – 200 bar equilibrium gas followed by Methane injection into a 2 block system; 0.125 mm punctured tin disc as the capillary break.

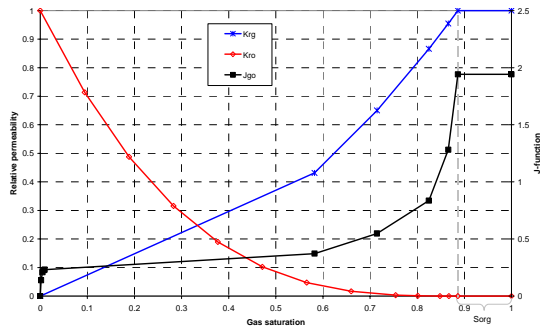


Figure 8: Relative permeabilities and J-function with  $S_{org}=0.114$ .

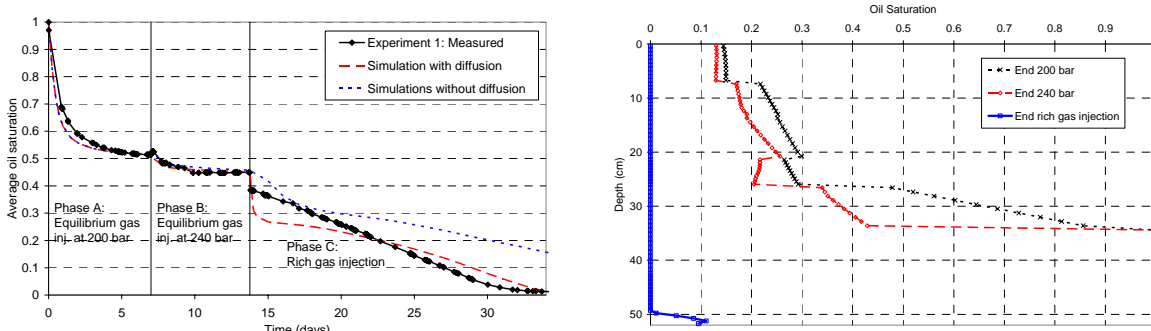


Figure 9: Simulation results from Experiment 1: Average oil saturation vs. time (left) and oil saturation vs. depth at end of each experimental phase from the simulation with diffusion (right).

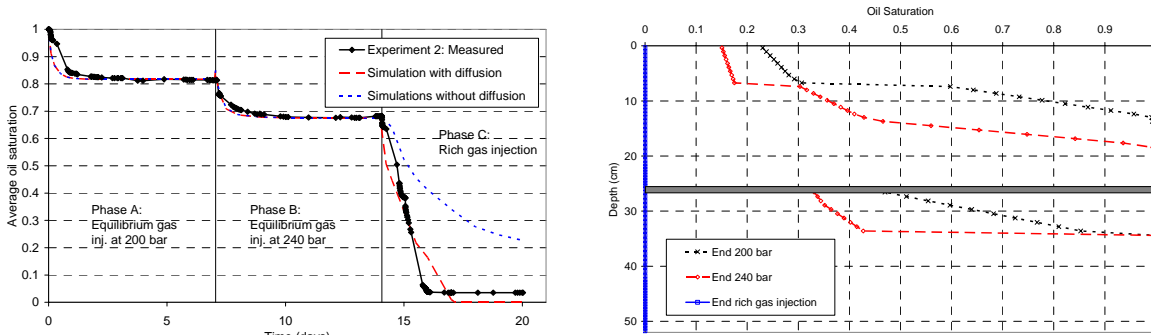


Figure 10: Simulation results from Experiment 2: Average oil saturation vs. time (left) and oil saturation vs. depth at end of each experimental phase from the simulation with diffusion (right).

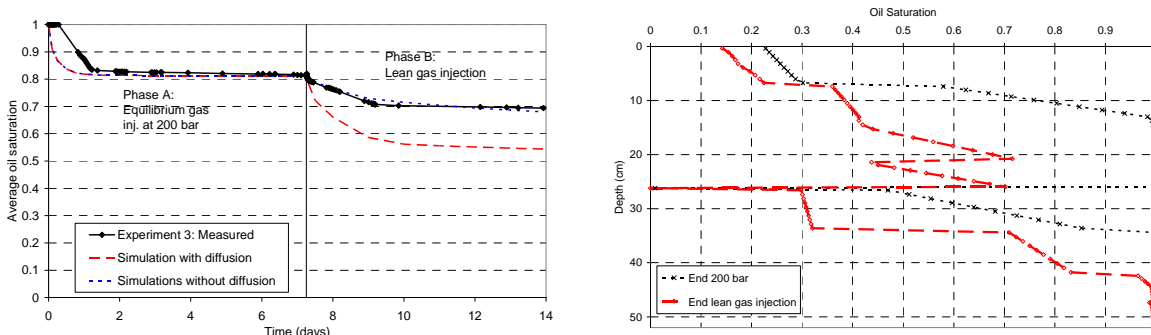


Figure 11: Simulation results from Experiment 3: Average oil saturation vs. time (left) and oil saturation vs. depth at end of each experimental phase from the simulation with diffusion (right).